# Gq signaling causes glomerular injury by activating TRPC6

Liming Wang,[1] Grant Jirka,[2] Paul B. Rosenberg,[3] Anne F. Buckley,[4,5] Jose A. Gomez,[3] Timothy A. Fields,[6] Michelle P. Winn,[1] and Robert F. Spurney[1]

[1]Division of Nephrology, Department of Medicine, Duke and Durham VA Medical Centers, Durham, North Carolina, USA. [2]Duke University, Durham, North Carolina, USA. [3]Division of Cardiology, Department of Medicine, Duke Medical Center, Durham, North Carolina, USA. [4]Department of Pathology, Duke University Medical Center, Durham, North Carolina, USA. [5]Duke Animal Pathology Core, Duke University, Durham, North Carolina, USA. [6]The Kidney Institute, University of Kansas Medical Center, Kansas City, Kansas, USA.

**Familial forms of focal segmental glomerulosclerosis (FSGS) have been linked to gain-of-function mutations in the gene encoding the transient receptor potential channel C6 (TRPC6). GPCRs coupled to Gq signaling activate TRPC6, suggesting that Gq-dependent TRPC6 activation underlies glomerular diseases. Here, we developed a murine model in which a constitutively active Gq α subunit ($Gq^{Q209L}$, referred to herein as GqQ>L) is specifically expressed in podocytes and examined the effects of this mutation in response to puromycin aminonucleoside (PAN) nephrosis. We found that compared with control animals, animals expressing GqQ>L exhibited robust albuminuria, structural features of FSGS, and reduced numbers of glomerular podocytes. Gq activation stimulated calcineurin (CN) activity, resulting in CN-dependent upregulation of TRPC6 in murine kidneys. Deletion of TRPC6 in GqQ>L-expressing mice prevented FSGS development and inhibited both tubular damage and podocyte loss induced by PAN nephrosis. Similarly, administration of the CN inhibitor FK506 reduced proteinuria and tubular injury but had more modest effects on glomerular pathology and podocyte numbers in animals with constitutive Gq activation. Moreover, these Gq-dependent effects on podocyte injury were generalizable to diabetic kidney disease, as expression of GqQ>L promoted albuminuria, mesangial expansion, and increased glomerular basement membrane width in diabetic mice. Together, these results suggest that targeting Gq/TRPC6 signaling may have therapeutic benefits for the treatment of glomerular diseases.**

## Introduction

GPCRs linked to Gq activation play a key role in glomerular diseases including receptors for angiotensin II (AT1), endothelins (ETA), thromboxanes (TP), cysteinyl-leukotrienes, and E-series prostaglandins (EP1) (1, 2). These cell surface GPCRs are found in podocytes and regulate pathways involved in cell survival, morphology, motility, and cellular attachment (1–6). As a result, GPCRs are important therapeutic targets for the treatment of glomerular disease processes. In this regard, AT1 receptor blockers (ARBs) are extensively used for the treatment of proteinuric kidney diseases (7–9), and combined therapy using ARBs and ETA blockers is currently being evaluated in clinical trials (10–12).

While the pathways activated by these GPCR systems are diverse, these receptors activate Gq α subunits (1). Gq stimulates phospholipase Cβ (PLCβ) and generates the second messengers diacyl glycerol (DAG) and inositol trisphosphates (IP3) (1). DAG is a potent activator of PKC (13), and several PKC isoforms play key roles in the pathogenesis of diabetic kidney disease (14). In contrast, IP3 mobilizes calcium from intracellular stores (13), and DAG and possibly inositol phosphates (IPs) promote activation of transient receptor potential channel C6 (TRPC6) in podocytes (1), which further enhances intracellular calcium levels. The importance of calcium in glomerular disease processes is highlighted by the observation that: (a) Gain-of-function mutations in *TRPC6* cause familial forms of focal segmental glomerulosclerosis (FSGS) (15, 16), and (b) TRPC6 is upregulated in primary glomerular diseases (17). Calcium, in turn, can activate additional signaling molecules including calcineurin (CN) (18). In the heart, Gq-dependent signaling cascades are potent activators of CN, and Gq-dependent CN activation promotes cardiac hypertrophy (19, 20) through mechanisms that involve, at least in part, CN-dependent upregulation of TRPC6 (21). In the kidney, CN regulates the stability of the podocyte cytoskeletal protein synaptopodin (SYN) (22) and promotes a decrease in the number of podocytes by mechanisms that are dependent on gene transcription and podocyte apoptosis (23, 24). Moreover, recent studies are consistent with the notion that Gq-dependent CN activation and, in turn, TRPC6 induction are relevant to podocyte biology in vivo (25–27).

To investigate the role of Gq signaling in the pathogenesis of glomerular diseases, we expressed a constitutively active Gq α subunit ($Gq^{Q209L}$, herein referred to as GqQ>L) specifically in podocytes in a doxycycline-inducible (DOX-inducible) fashion (28). As previously reported, induction of GqQ>L does not cause glomerular injury (28), suggesting that a "second hit" may be required to induce podocyte injury, as has been suggested for

**Note regarding evaluation of this manuscript:** Manuscripts authored by scientists associated with Duke University, The University of North Carolina at Chapel Hill, Duke-NUS, and the Sanford-Burnham Medical Research Institute are handled not by members of the editorial board but rather by the science editors, who consult with selected external editors and reviewers.

**Conflict of interest:** The authors have declared that no conflict of interest exists.

**Submitted:** April 24, 2014; **Accepted:** February 27, 2015.

**Reference information:** *J Clin Invest*. 2015;125(5):1913–1926. doi:10.1172/JCI76767.

**Table 1. Effect of PAN nephrosis on glomerular structure**

| | Podocytes per glomerular profile | V/glom ($\times 10^5$ $\mu m^3$) | Nv(P/glom) ($\times 10^{-5}$/$\mu m^3$) |
|---|---|---|---|
| Untreated controls ($n$ = 11) | 8.74 ± 0.28 | 2.34 ± 0.14 | 56.8 ± 1.7 |
| PAN controls ($n$ = 9) | 8.70 ± 0.19 | 2.82 ± 0.02 | 49.7 ± 2.2 |
| PAN GqQ>L ($n$ = 13) | 6.91 ± 0.6[A] | 2.73 ± 0.15 | 42.4 ± 3.7[B] |

[A]$P < 0.05$ versus controls and PAN controls; [B]$P < 0.01$ versus untreated controls. V/glom, glomerular volume; Nv(P/glom), podocyte density.

some familial forms of FSGS (29) such as activating mutations in *TRPC6* (30). We therefore determined whether Gq activation in podocytes exacerbated glomerular injury in nephrosis induced by the podocyte toxin puromycin aminonucleoside (PAN) (31). We found that treatment with PAN induced robust albuminuria, foot process (FP) effacement, a decrease in the number of glomerular podocytes, and light microscopic features of FSGS in mice expressing GqQ>L specifically in podocytes compared with what was observed in control animals. These adverse effects were associated with both CN activation in vivo and enhanced expression of TRPC6. Deletion of *Trpc6* prevented the development of FSGS and podocyte loss in this model. Similarly, CN blockade with FK506 reduced proteinuria and preserved podocyte numbers but had more modest effects on glomerular and tubular histology. These data support the notion that components of the Gq/TRPC6 signaling cascade are important therapeutic targets for the treatment of glomerular disease processes. Moreover, the data support the concept that a second hit may be required for the development of some familial forms of FSGS such as gain-of-function mutations in *TRPC6*.

## Results

To evaluate the role of Gq-coupled signaling cascades in promoting podocyte injury, we expressed a constitutively active Gq α subunit (GqQ>L) specifically in glomerular podocytes in a DOX-inducible fashion (28). As shown in Supplemental Figure 1A (supplemental material available online with this article; doi:10.1172/JCI76767DS1), this system requires 2 transgenic (Tg) animals (32). The first Tg animal expresses reverse tetracycline transactivator (*rtTA*) under the control of the human podocin promoter (*NPHS2*) to create *NPHS2-rtTA* mice (33). The second Tg mouse expresses GqQ>L under the control of tet operator sequence (*tetO*) and a minimal CMV promoter (PminCMV) to create *tetO*-GqQ>L mice (32). By breeding the 2 Tg mice, animals were obtained that expressed both transgenes. In these "double-Tg" mice (*NPHS2-rtTA tetO*-GqQ>L mice, herein referred to as GqQ>L mice), treatment with DOX induced transgene expression. For the studies, we used GqQ>L mice as well as their littermate controls (single-Tg and non-Tg animals), which do not express GqQ>L in the presence of DOX (28). At 3 to 4 months of age, the mice were treated with DOX for 1 week and then received 1 dose of PAN as previously described (34). The mice were then studied as discussed in the Methods.

As shown in Figure 1A and Supplemental Figure 1B, treatment with DOX and PAN induced robust albuminuria following induction of GqQ>L. As shown in Figure 1, B and C, this increase in albuminuria was associated with the development of FSGS in approximately one-third of mice expressing GqQ>L ($P < 0.05$) as well as of tubular dilation and casts (Figure 1D), which tended to be more severe in GqQ>L mice (Supplemental Figure 1C). These histologic abnormalities were accompanied by a decrease in both the number of glomerular podocytes and podocyte density in GqQ>L mice compared with either untreated controls or controls treated with DOX and PAN (Figure 1E and Table 1) as well as reduced expression of both SYN and WT1 in glomerular preparations as shown by immunoblot analysis (Figure 1, F and G). As previously reported (28), induction of GqQ>L by DOX had no effect on albuminuria or glomerular histology in the absence of PAN treatment (Supplemental Figure 2, A and B), despite efficient expression of the transgene (Supplemental Figure 2C).

Gq activates the serine/threonine phosphatase CN by stimulating an increase in intracellular calcium levels (28). CN activation promotes podocyte injury (23, 24, 35), and these adverse effects are likely mediated in part by dephosphorylation of nuclear factor of activated T cells (NFAT) (23, 24). We therefore determined whether GqQ>L induction in vivo stimulated CN activity using CN reporter mice (36). For these studies, we bred GqQ>L mice with mice expressing an NFAT reporter construct linked to β-gal induction. This created "triple" Tg mice, which express GqQ>L following DOX treatment, and either "single" Tg mice (NFAT reporter mice, *NPHS2-rtTA* mice, and *tetO*-GqQ>L mice) or "double" Tg mice (TG NFAT reporter *NPHS2-rtTA* mice, NFAT reporter *tetO*-GqQ>L mice, and GqQ>L mice), which either do not express GqQ>L or lack the NFAT reporter construct or both (labeled "other" Tg). We also bred non-Tg mice for use as an additional control. As shown in Figure 2A, treatment with DOX activated the NFAT reporter construct in renal cortices from triple-Tg animals (NFAT reporter GqQ>L mice), with lesser activation in other organ systems and little background activation in either "other" Tg or non-Tg mice. We also evaluated β-gal activity in enriched glomerular preparations from each experimental group in the presence of DOX or sucrose vehicle. As shown in Figure 2B, induction of GqQ>L with DOX caused robust activation of the reporter construct compared with vehicle-treated mice, with little activation of the reporter construct in the presence or absence of DOX in the other experimental groups.

An important gene target of NFAT transcription factors is the ion channel TRPC6 (21). In the heart, CN stimulates cardiac hypertrophy (19, 20), and this hypertrophic effect is mediated in part by enhanced expression of TRPC6 (21). Moreover, recent studies suggest that this pathway is relevant to podocyte biology (26, 27, 37). To determine whether GqQ>L induction enhanced TRPC6 expression by CN-dependent mechanisms, we first determined whether DOX treatment induced *Trpc6* mRNA in GqQ>L mice. As shown in Figure 3, A and B, GqQ>L enhanced expression of *Trpc6* mRNA in enriched glomerular preparations, and this increase in *Trpc6* mRNA levels was inhibited by the pharmacological CN inhibitor FK506. We next determined the effect of GqQ>L induction by immunoblotting glomerular preparations. As shown in Figure 3, C and D, induction of GqQ>L expression by DOX enhanced TRPC6 protein levels compared with those in controls, and this increase was attenuated by FK506.

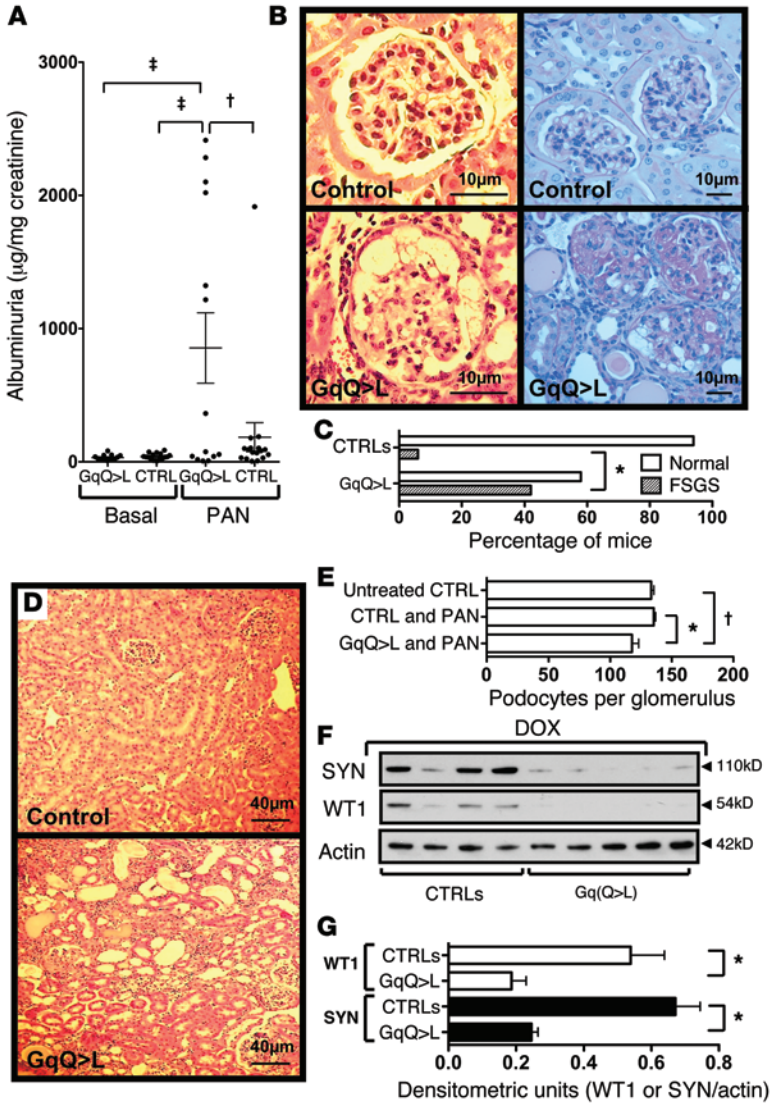


**Figure 1. Effect of GqQ>L induction on PAN nephrosis.** (**A**) PAN caused a significant increase in albuminuria in mice expressing GqQ>L. There was significantly less albuminuria induced by PAN in control mice (CTRL) than in GqQ>L mice. (**B** and **C**) Treatment with PAN caused a significant increase in the percentage of mice that developed FSGS. Cystic structures were seen in a few glomeruli in GqQ>L mice (**B**, lower left panel), which likely indicates the accumulation of lipids or proteins in the cytoplasm of epithelial cells. Scale bars: 10 μm. (**D**) Treatment with PAN induced tubule dilation and casts in GqQ>L mice. Scale bars: 40 μm. (**E**) Podocyte numbers were significantly reduced by treatment with PAN in GqQ>L mice compared with numbers in both control mice treated with PAN and untreated control mice. (**F** and **G**) Treatment with PAN caused a significant decrease in both SYN and WT1 expression in GqQ>L mice. For albuminuria and the histologic studies, 17 control and 14 GqQ>L mice were used. Four controls and 5 GqQ>L mice were used for the immunoblotting experiments. To assess podocyte numbers, samples from 11 untreated controls, 9 controls treated with PAN, and 13 GqQ>L mice treated with PAN were used. $^{*}P < 0.05$, $^{\dagger}P < 0.01$, and $^{\ddagger}P < 0.005$ versus the indicated groups by Fisher's exact test for histologic data and by ANOVA, followed by Bonferroni's post-hoc analysis, for the other studies.

To determine whether TRPC6 plays a role in podocyte injury, we generated GqQ>L mice lacking TRPC6. For these studies, controls, *Trpc6*$^{+/+}$ GqQ>L mice, and *Trpc6*$^{-/-}$ GqQ>L mice (herein referred to as *Trpc6*-KO GqQ>L mice) were treated with DOX and PAN, as described in the Methods. As demonstrated in Figure 4A and Supplemental Figure 3A, PAN-induced albuminuria was significantly increased in *Trpc6*$^{+/+}$ GqQ>L mice compared with that seen in either baseline or wild-type (WT) controls treated with PAN. In *Trpc6*-KO GqQ>L mice, albuminuria induced by PAN was significantly decreased compared with *Trpc6*$^{+/+}$ GqQ>L mice treated with PAN. Moreover, the absence of TRPC6 completely prevented the development of FSGS in *Trpc6*-KO GqQ>L mice (Figure 4, B and D). Similarly, tubular injury (dilation and casts) was significantly attenuated in GqQ>L mice lacking TRPC6 compared with *Trpc6*$^{+/+}$ GqQ>L mice (Figure 4, C and E). Tubulointerstitial (TI) inflammation and fibrosis also tended to be decreased by KO of *Trpc6*, but these differences did not reach statistical significance ($P = 0.07$) (Supplemental Figure 3B). As shown in Figure 4F, these light microscopic findings were associated with a decrease in the number of glomerular podocytes in *Trpc6*$^{+/+}$ GqQ>L mice compared with WT controls, and this decrease in podocyte numbers was prevented by KO of *Trpc6* (*Trpc6*-KO GqQ>L) in mice. A similar pattern was observed when data were expressed as podocyte density (Table 2). Moreover, expression of both SYN and WT1 proteins was preserved by KO of *Trpc6* (Figure 4, G and H). As shown in Supplemental Figure 4A, the decrease in SYN protein levels in *Trpc6*$^{+/+}$ GqQ>L mice treated with PAN was associated with an increase in *Syn* mRNA levels. In contrast, SYN protein levels in *Trpc6*-KO GqQ>L mice were preserved without an increase in *Syn* mRNA expression. Systolic BP (SBP) was similar in *Trpc6*$^{+/+}$ GqQ>L and *Trpc6*-KO GqQ>L mice (127 ± 3 [WT] vs. 129 ± 3 [KO]; $P$ = NS).

Quantitative RT-PCR (qRT-PCR) was used to investigate the effect of GqQ>L induction on the CN-responsive genes *Trpc6*, regulator of CN 1 (*Rcan1*), and cyclooxygenase 2 (*Cox2*) (21, 28). As shown in Figure 4I, *Cox2* mRNA was significantly increased in GqQ>L mice compared with levels in controls. Similarly, both *Trpc6* and *Rcan1* tended to be increased in GqQ>L mice compared with controls (Figure 4, I and J). KO of *Trpc6* significantly reduced expression of *Cox2* mRNA in GqQ>L mice. Similarly, *Rcan1* tended to be decreased in *Trpc6*-KO mice compared with *Trpc6*$^{+/+}$ GqQ>L mice. A signal for *Trpc6* was not detected in the *Trpc6*-KO mice (Figure 4J). Last, we investigated the effect of TRPC6 on expression of the other TRPC family members *Trpc3* and *Trpc5*. As shown in Supplemental Figure 5, *Trpc3* mRNA levels tended to be increased in *Trpc6*$^{+/+}$ GqQ>L mice treated with PAN, similar to that seen in to mice treated with angiotensin II (AII) (37). In contrast, *Trpc3* mRNA levels were significantly decreased in *Trpc6*-KO GqQ>L mice compared with those in *Trpc6*$^{+/+}$ GqQ>L mice. Given that KO of *Trpc6* may have decreased cytosolic calcium levels, these observations could be consistent with the known stimulatory effects of calcium signal-

**Table 2. Effect of *Trpc6* KO on glomerular structure**

| | Podocytes per glomerular profile | V/glom ($\times 10^5$ μm$^3$) | Nv(P/glom) ($\times 10^{-5}$/μm$^3$) |
|---|---|---|---|
| PAN controls ($n$ = 9) | 8.29 ± 0.17 | 2.59 ± 0.08 | 48.7 ± 0.7 |
| PAN GqQ>L ($n$ = 9) | 6.90 ± 0.33[A] | 2.47 ± 0.21 | 43.2 ± 1.5[B] |
| PAN *Trpc6* KO ($n$ = 9) | 7.67 ± 0.36 | 2.46 ± 0.22 | 47.8 ± 1.4 |

[A]$P < 0.05$ versus PAN controls; [B]$P < 0.05$ versus PAN controls or PAN *Trpc6*-KO.

ing on TRPC3 expression (38). TRPC5 levels were not significantly different in the experimental groups.

The effects of GqQ>L on glomerular ultrastructure in *Trpc6*$^{+/+}$ GqQ>L and *Trpc6*-KO GqQ>L mice are shown in Figure 5, A and B. FP effacement was observed in all experimental groups treated with PAN and was qualitatively more severe in *Trpc6*$^{+/+}$ GqQ>L mice (Figure 5A). Consistent with the qualitative impression, the frequency of filtration slits was significantly decreased in *Trpc6*$^{+/+}$ GqQ>L mice compared with the frequency in either WT controls or *Trpc6*-KO GqQ>L mice (Figure 5B). In *Trpc6*$^{+/+}$ GqQ>L mice, the glomerular ultrastructure was markedly abnormal, with amorphous material in the capillary loops, focal capsular adhesions, and widespread degenerative changes in the podocytes and capillary loop endothelial cells. Microvillous changes were observed in a few of the *Trpc6*$^{+/+}$ GqQ>L and *Trpc6*-KO GqQ>L mice.

KO of *Trpc6* may reduce kidney injury by attenuating Gq-mediated increases in intracellular calcium and, in turn, decreasing enzymatic activity of the calcium-activated phosphatase CN. We therefore determined whether the CN inhibitor FK506 reduced glomerular injury in the GqQ>L mice treated with PAN. For these studies, the GqQ>L transgene was induced by DOX for 1 week, and then mice received 1 dose of PAN, followed by daily injections of either the CN inhibitor FK506 or vehicle, as described in the Methods. As shown in Figure 6A and Supplemental Figure 6A, FK506 reduced albuminuria in GqQ>L mice compared with that observed in vehicle-treated GqQ>L mice. FK506 had more modest and nonsignificant effects on the development of FSGS (Figure 6, B and C) and TI inflammation and fibrosis (Supplemental Figure 6B), although there was a significant reduction in tubule injury (Figure 6, D and E). The beneficial effects of CN blockade were associated with a significant increase in podocyte density (Table 3) and preservation of SYN protein levels (Figure 6, F and G), without significantly affecting podocyte numbers (Figure 6H). As shown in Supplemental Figure 4B, *Syn* mRNA levels tended to be increased in both vehicle- and FK506-treated GqQ>L mice compared with those in controls. We were unable to detect a significant effect of WT1 levels by immunoblotting. As shown in Figure 6I, FK506 tended to reduce expression of the CN-responsive genes *Ttrpc6* and *Rcan1*. In contrast, the increase in *Cox2* mRNA caused by induction of GqQ>L (Figure 4I) was not affected by FK506 (Figure 6J) as previously reported (28).

The renin-angiotensin system has been suggested to be a disease accelerant in rodent models of diabetic kidney disease (39, 40). In support of this hypothesis, overexpression of a renin transgene was found to promote the development of advanced diabetic kidney disease in Tg rats (39). The enzyme renin initiates an endocrine cascade that results in the generation of the effector peptide AII and in turn activates the Gq-coupled AT1 receptor (39). Thus, Gq-coupled signaling cascades may provide the second hit that augments kidney damage in rodent models of diabetes. To determine whether the adverse effects of podocyte Gq activation are generalizable to other glomerular disease processes, we determined whether induction of GqQ>L exacerbated diabetic kidney disease in a mouse model of type 1 diabetes (FVB/NJ Akita mice) (41). As shown in Figure 7A, podocyte-specific expression of GqQ>L enhanced albuminuria in Akita mice (Gq Akita mice) at 16 and 20 weeks of age. Enhanced albuminuria was associated with a significant increase in mesangial expansion (Figure 7, B and C) in either a diffuse (Figure 7B, middle panel) or nodular (Figure 7B, right panel) pattern. The glomerular ultrastructure is shown in Figure 7D. Nodular thickening of the glomerular basement membrane (GBM) was seen on the subepithelial surface in Gq Akita mice, which was associated with a significant increase in average GBM width compared with that seen in age- and sex-matched nondiabetic control group mice (Figure 7E). Focal areas of FP flattening were also observed, which was qualitatively more severe in the diabetic mice (Figure 7D and Supplemental Figure 7). As shown in Figure 7F, there was a significant increase in total collagen content in WT and Gq Akita mice compared with that in the nondiabetic control group. Collagen content tended to be increased in the Gq Akita group compared with WT Akita mice, but this difference was not statistically significant ($P < 0.10$). Tubular and interstitial injury was similar in both groups by light microscopic examination (Supplemental Figure 8, A and B). Table 4 shows the effects of diabetes on glomerular volume, podocyte density, and podocyte numbers. Glomerular volume and podocyte density were similarly increased and decreased, respectively, in both groups of Akita mice compared with mice in the nondiabetic age- and sex-matched control group. Podocyte numbers also tended to be reduced in both groups of Akita mice, but this difference was not statistically significant.

We next investigated the effect of diabetes and GqQ>L induction on the CN-responsive genes *Trpc6*, *Cox2*, and *Rcan1*. As shown in Figure 7G, both *Trpc6* and *Cox2* tended to be increased in WT and Gq Akita mice compared with age-matched nondiabetic controls. These differences were statistically significant for *Trpc6* and *Cox2* in the WT and Gq Akita groups, respectively. As shown in Figure 7H, *Rcan1* levels were markedly increased in WT Akita mice compared with levels detected in controls. *Rcan1* was also increased ≈3-fold in Gq Akita mice compared with controls,

**Table 3. Effect of FK506 on glomerular structure**

| | Podocytes per glomerular profile | V/glom ($\times 10^5$ μm$^3$) | Nv(P/glom) ($\times 10^{-5}$/μm$^3$) |
|---|---|---|---|
| Untreated controls ($n$ = 11) | 8.52 ± 0.17 | 2.46 ± 0.09 | 52.9 ± 0.5[B] |
| PAN vehicle ($n$ = 13) | 6.67 ± 0.42[A] | 2.44 ± 0.24 | 31.0 ± 6.2 |
| PAN FK506 ($n$ = 18) | 7.18 ± 0.35 | 1.90 ± 0.23[A] | 48.4 ± 2.3[B] |

[A]$P < 0.05$ versus untreated controls; [B]$P < 0.01$ versus GqQ>L mice treated with PAN and vehicle.

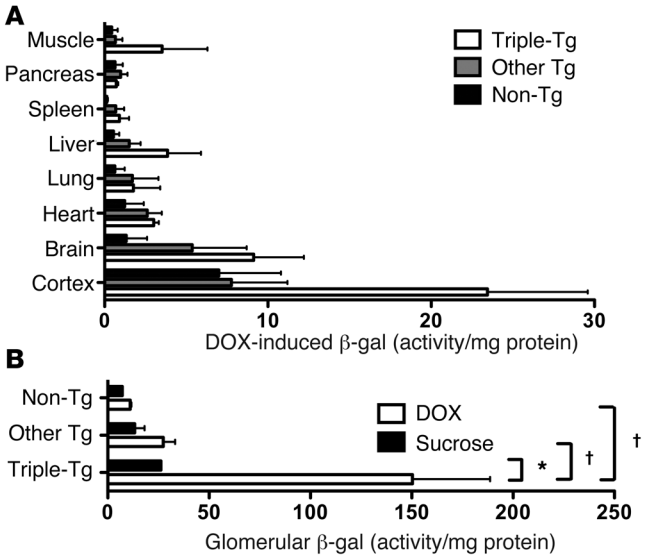


**Figure 2. Activation of an NFAT reporter construct in GqQ>L mice.** (**A**) In GqQ>L mice expressing the NFAT reporter construct (triple-Tg mice), induction of GqQ>L activated the reporter construct in kidney cortex compared with both other-Tg (double- and single-Tg) and non-TG mice, with lesser activation in the other tissues examined. (**B**) Treatment with DOX caused robust activation of the NFAT reporter construct in glomerular preparations from triple-Tg mice compared with that seen in sucrose-treated triple-Tg mice. For the experiments, 3 mice were studied in each group. $^{*}P < 0.05$ or $^{\dagger}P < 0.01$ versus the indicated groups using ANOVA, followed by a Bonferroni's post-hoc test.

but this difference was not statistically significant and was significantly attenuated compared with *Rcan1* levels in the WT Akita group ($P < 0.01$). Both blood glucose and glycated albumin levels were similarly elevated in the WT and Gq Akita groups (Supplemental Figure 9).

## Discussion

In the present studies, we found that podocyte-specific activation of Gq in PAN nephrosis promoted albuminuria, reduced the number of glomerular podocytes, and induced FSGS. KO of *Trpc6* both inhibited podocyte loss and completely prevented FSGS induced by PAN nephrosis in GqQ>L mice. These data suggest that TRPC6 is a key downstream target activated by Gq signaling that promotes podocyte injury. Intriguingly, glomerular damage induced by Gq required a second hit (ref. 28 and Supplemental Figure 2). Indeed, a second hit may be required for the development of glomerular disease in some familial forms of FSGS (29). In this regard, the age at diagnosis is quite broad in patients with FSGS caused by gain-of-function mutations in *TRPC6* (15, 16, 42), consistent with the idea that some type of environmental or genetic second hit may be required for the development of glomerular disease (30). In support of this possibility, Gigante et al. (43) described *TRPC6* mutations in patients with early-onset nephrotic syndrome. In 2 patients, *TRPC6* mutations resulted in an amino acid (N125S) change that had previously been reported in patients with adult-onset FSGS (43). These 2 patients were, however, compound heterozygotes for both the *TRPC6* (N125S) mutation and a mutation in nephrin (*NPHS1* R831C) that had previously been reported to cause the autosomal recessive disease congenital nephropathy of the Finnish type. Thus, the mutant *NPHS1* allele may have accelerated disease in the pediatric patients with the *TRPC6* (N125S) mutation. The concept of a second hit promoting disease progression is further supported by a recent study of autosomal recessive steroid-resistant nephrotic syndrome due to mutations in the *NPHS2* gene encoding podocin (44). In this study, the authors suggested that the pathogenicity of 1 *NPHS2* allele (R229Q) was dependent on a transassociated mutation in the other allele that caused a different amino acid change, consistent with the idea that a genetic second hit was required to develop a disease phenotype.

In the present study, Gq-dependent TRPC6 activation did not cause glomerular damage in the absence of an additional cell stressor. In this regard, PAN stimulates ROS generation in podocytes (45), and ROS potently activate TRPC6 (46, 47). Moreover, Gq-coupled GPCRs stimulate TRPC6 activation, both directly through the second messengers DAG and possibly IP3 (1), as well as indirectly by stimulating ROS generation (48). In this scenario, TRPC6 may serve as a final common pathway causing podocyte injury by several injury-promoting signaling cascades. These data suggest that, while we often study mediators of glomerular damage as individual entities, it is likely that the biological outcome represents the net effect of the number of injury-promoting pathways activated, the magnitude of activation of each individual mediator, and the genetic predisposition of the individual. Thus, treatment strategies that are currently used for idiopathic forms of FSGS may have beneficial effects in genetic forms of the disease by limiting the number of injury-promoting pathways that contribute to disease progression.

Current treatments for proteinuric kidney diseases include the use of therapies targeting the renin-angiotensin system. Given that these agents inhibit activation of the Gq-coupled AT1 receptor (1), the beneficial effects of the renin-angiotensin sys-

**Table 4. Effect of GqQ>L on glomerular structure in Akita mice**

| | Podocytes per glomerular profile | V/glom ($\times 10^5$ μm$^3$) | Nv(P/glom) ($\times 10^{-5}$/μm$^3$) | Podocytes per glomerulus |
|---|---|---|---|---|
| Nondiabetic controls ($n$ = 6) | 8.76 ± 0.27 | 2.57 ± 0.09 | 56.8 ± 1.7 | 144 ± 4.5 |
| WT Akita ($n$ = 9) | 8.35 ± 0.28 | 3.61 ± 0.17$^{A}$ | 38.3 ± 1.3$^{B}$ | 135 ± 3.5 |
| Gq Akita ($n$ = 8) | 8.47 ± 0.23 | 3.56 ± 0.26$^{A}$ | 39.4 ± 0.9$^{B}$ | 136 ± 3.4 |

$^{A}P < 0.01$ or $^{B}P < 0.001$ versus nondiabetic controls.

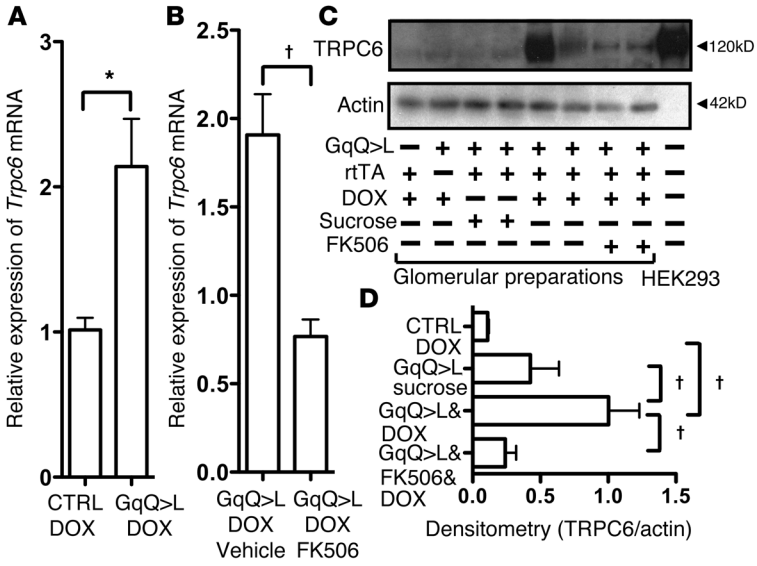


**Figure 3. Induction of GqQ>L in podocytes enhances TRPC6 expression in vivo.** (**A**) Treatment with DOX enhanced *Trpc6* mRNA levels in glomerular preparations from GqQ>L mice compared with levels detected in controls. (**B**) FK506 inhibited expression of *Trpc6* mRNA in glomerular preparations from GqQ>L mice treated with DOX. (**C** and **D**) TRPC6 expression was similar in controls treated with DOX and in GqQ>L mice treated with sucrose. Treatment with DOX enhanced TRPC6 expression in GqQ>L mice compared with expression in either controls treated with DOX or in GqQ>L mice treated with sucrose. Induction of TRPC6 protein in GqQ>L mice treated with DOX was blocked by FK506. Actin was used as a loading control, and HEK293 cells transfected with a TRPC6 construct were used as a positive control for the immunoblotting studies. Because of the high levels of TRPC6 expression in the HEK293 cells, small amounts of the HEK293 cell lysate were used, and the actin loading control was not visible at this length of exposure. For the qRT-PCR analysis, 11 controls treated with DOX, 4 GqQ>L mice treated with DOX, 8 GqQ>L mice treated with DOX and vehicle, and 4 GqQ>L mice treated with DOX and FK506 were used. For the immunoblotting studies, 4 controls treated with DOX, 4 GqQ>L mice treated with sucrose, 4 GqQ>L mice treated with DOX, and 4 GqQ>L mice treated with DOX and FK506 were used. $^{*}P < 0.025$ or $^{\dagger}P < 0.01$ versus the indicated groups using a 2-tailed *t* test for qRT-PCR data and ANOVA, followed by a Bonferroni's post-hoc test, for densitometric data.

tem blockade in glomerular diseases may be mediated at least in part by inhibition of Gq signaling. In support of this hypothesis, multiple Gq-coupled GPCRs contribute to kidney injury in animal models of glomerular disease including receptors for ETA, TP, platelet-activating factor (PAF), cysteinyl leukotrienes, and EP1 (1, 5). Moreover, combined use of AT1 and ETA blockers is a promising treatment for glomerular diseases (10–12). An alternative treatment strategy might be to target a final common pathway activated by each of these receptor systems such as Gq α subunits. YM254890 is a specific Gq inhibitor that has been tested in experimental animals (49–51). In these studies, YM254890 reduced systemic BP and inhibited platelet aggregation without apparent adverse effects. While additional studies will be required to determine the effects of YM254890 in proteinuric kidney diseases, the current studies suggest that this class of agents may have beneficial actions in glomerular disease processes, which might be useful for the treatment of kidney diseases in humans.

Other therapeutic strategies include targeting downstream signaling cascades linked to Gq activation. TRPC6 is stimulated by Gq through generation of the second messenger DAG and possibly IP3 (1). These signaling molecules are products of PLC following activation of either Gq-coupled GPCRs or RTKs (52), and both these receptor systems play key roles in glomerular disease processes (1, 53). Activation of TRPC6 increases cytosolic calcium levels and stimulates Rho A (3, 4). Moreover, Gq-coupled signaling cascades activate other TRPC family members including TRPC5 (54), which further enhances intracellular calcium levels and promotes RAC1 activation (3, 4). Both Rho A and RAC1 modulate cytoskeletal dynamics and play critical roles in regulating glomerular filtration barrier integrity (3, 55–59). Gq signaling also stimulates CN (26, 60) and causes a decrease in glomerular podocytes by mechanisms that are dependent on gene transcription (23, 24). In this regard, Gq-dependent CN activation induced TRPC6 expression (21) without affecting *Trpc5* mRNA levels (Supplemental Figure 5). This increase in TRPC6 expression causes additional increases in intracellular calcium levels and augments Rho A activation (3, 4). Thus, Gq signaling stimulates multiple signaling cascades (Rho GTPases and CN) that might be targeted to promote podocyte survival and glomerular filtration barrier integrity.

Another therapeutic strategy is CN inhibition (29). Pharmacological CN inhibitors are frequently used for the treatment of primary glomerular disease processes (29, 61). While the beneficial effects of these agents have been attributed to their immunological actions (62), accumulating evidence suggests that this calcium-activated phosphatase has important nonimmunological effects in glomerular diseases, including promoting degradation of the podocyte cytoskeletal protein SYN (22, 62), as well as inducing podocyte apoptosis and podocyte loss (23, 24). In the present studies, GqQ>L induction both activated CN and upregulated TRPC6 in a CN-dependent fashion. These observations may be relevant to kidney pathophysiology, because TRPC6 is induced in several primary glomerular diseases (17). We therefore determined whether the CN inhibitor FK506 attenuated glomerular injury induced by PAN in GqQ>L mice. We found that FK506 attenuated both albuminuria and tubular injury induced by GqQ>L in PAN nephrosis as well as enhanced expression of SYN. Despite these beneficial effects, FK506 had little effect on glomerular histology. The dissociation between effects on proteinuria and renal injury is consistent with several clinical studies suggesting that treatments that inhibit proteinuria do not necessarily translate into reduced disease progression (11, 63). Our findings of the inability of CN inhibition to improve renal histology should, however, be tempered by the observation that current pharmacological CN inhibitors have important off-target effects (64). For example, CN inhibitor therapy has been linked to the development of FSGS in some patients, perhaps by promoting renal ischemia (29, 65). In support of this hypothesis, glomerular volume was reduced in GqQ>L mice treated with FK506 (Table 3), consistent with the idea that FK506 caused renal ischemia and, in turn, a reduction in glomerular volume (66). Moreover, FK506 had little effect on GqQ>L-dependent induction of COX2 (Figure 6J). Indeed, in previous studies, we found that FK506-induced expres-

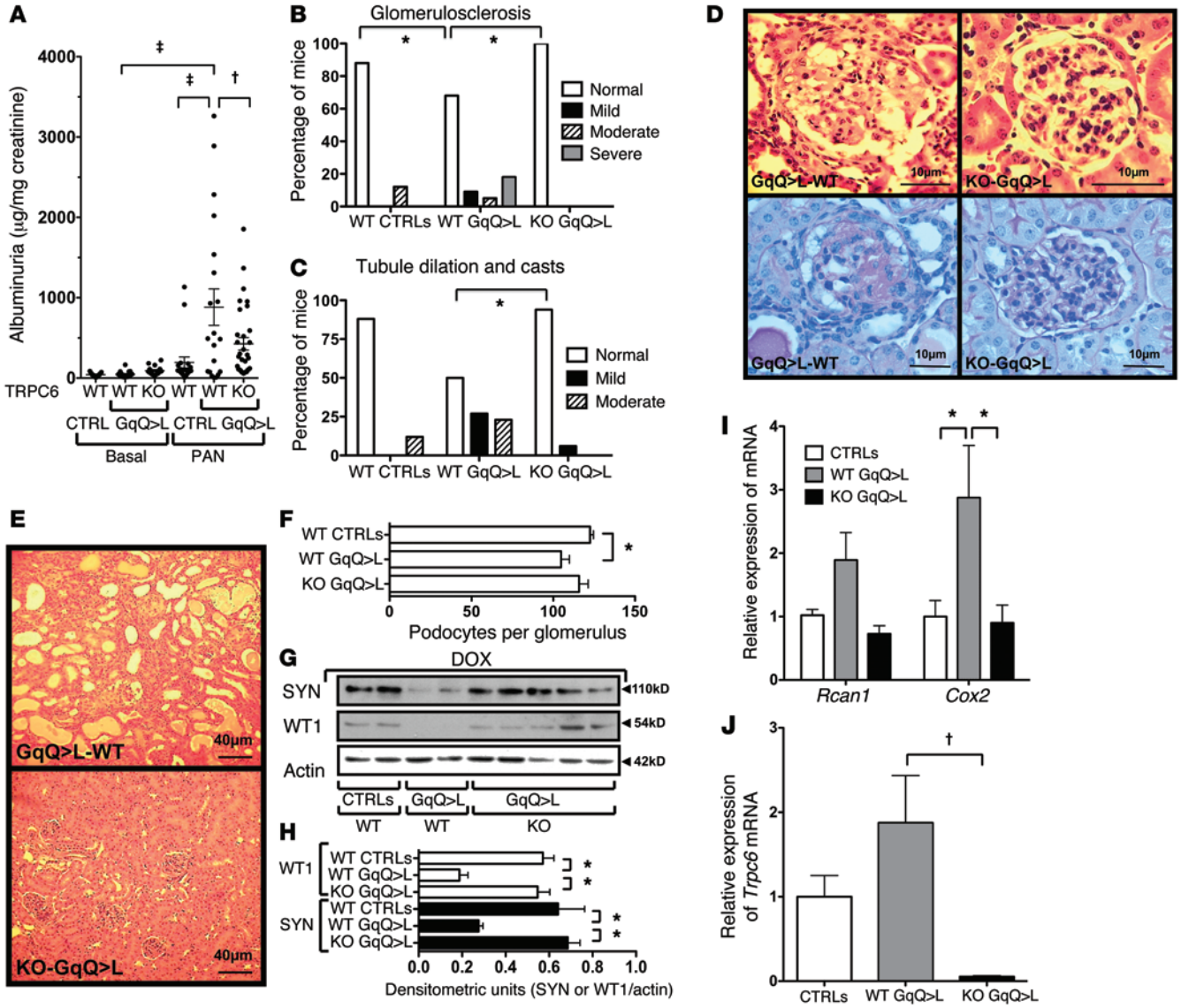


**Figure 4. Effect of *Trpc6*-KO on PAN nephrosis.** (**A**) Albuminuria was increased in *Trpc6*$^{+/+}$ GqQ>L mice. KO of *Trpc6* attenuated the increase in albuminuria. (**B** and **D**) FSGS was increased in *Trpc6*$^{+/+}$ GqQ>L mice. KO of *Trpc6* prevented the development of FSGS. Scale bars: 10 μm. (**C** and **E**) Tubule dilation and casts were reduced by KO of *Trpc6*. Scale bars: 40 μm. (**F**) Treatment with PAN reduced podocyte numbers in *Trpc6*$^{+/+}$ GqQ>L mice. Podocyte numbers in *Trpc6*-KO mice were similar to those in WT controls. (**G** and **H**) KO of *Trpc6* preserved expression of SYN and WT1 in GqQ>L mice. (**I** and **J**) *Cox2* mRNA was increased in *Trpc6*$^{+/+}$ GqQ>L mice, and this increase was prevented by KO of *Trpc6*. A similar pattern was observed for *Rcan1* and *Trpc6* mRNA levels. The albuminuria experiments were performed in 15 WT controls, 20 *Trpc6*$^{+/+}$ GqQ>L mice, and 26 *Trpc6*-KO GqQ>L mice. For the histology studies, 8 WT controls, 22 *Trpc6*$^{+/+}$ GqQ>L mice, and 16 *Trpc6*-KO GqQ>L mice were used. To assess podocyte numbers, 9 WT controls, 9 *Trpc6*$^{+/+}$ GqQ>L mice, and 9 *Trpc6*-KO GqQ>L mice were used. For immunoblotting experiments, 4 controls, 4 *Trpc6*$^{+/+}$ GqQ>L mice, and 10 *Trpc6*-KO GqQ>L mice were used. For qRT-PCR, mRNA samples from 12 WT controls, 17 *Trpc6*$^{+/+}$ GqQ>L mice, and 10 *Trpc6*-KO GqQ>L mice were used. $^{*}P < 0.05$, $^{\dagger}P < 0.01$, or $^{\ddagger}P < 0.005$ versus the indicated groups using a $\chi^2$ analysis for histologic data and ANOVA, followed by Bonferroni's post-hoc analysis, for the other studies. KO GqQ>L, *Trpc6*-KO GqQ>L mice; WT GqQ>L, *Trpc6*$^{+/+}$ GqG>L mice.

sion of *Cox2* mRNA (28) and enhanced generation of COX2 metabolites may contribute to CN inhibitor toxicity (65). The development, however, of more specific CN inhibitors with fewer off-target effects may provide the benefits of CN blockade with a more favorable side-effect profile (67, 68). In future studies, it will therefore be of interest to test the effects of these more specific CN inhibitors in glomerular disease processes.

Although FK506 did not affect glomerular pathology, tubule dilation and casts were reduced with CN inhibitor therapy. While the mechanisms of this effect cannot be known with certainty, Dong and coworkers (69) reported that CN inhibitors attenuate renal tubular cell (RTC) apoptosis induced by either ischemia or azide-dependent ATP depletion by inhibiting dephosphorylation of the CN substrate dynamin-related protein 1 (DRP1) and by blocking mitochondrial fragmentation and, in turn, RTC apoptosis. Similarly, excessive urinary protein levels promote RTC apoptosis through the mitochondrial apoptotic pathway (70). Thus, it is possible that loss of glomerular filtration barrier integrity indi-

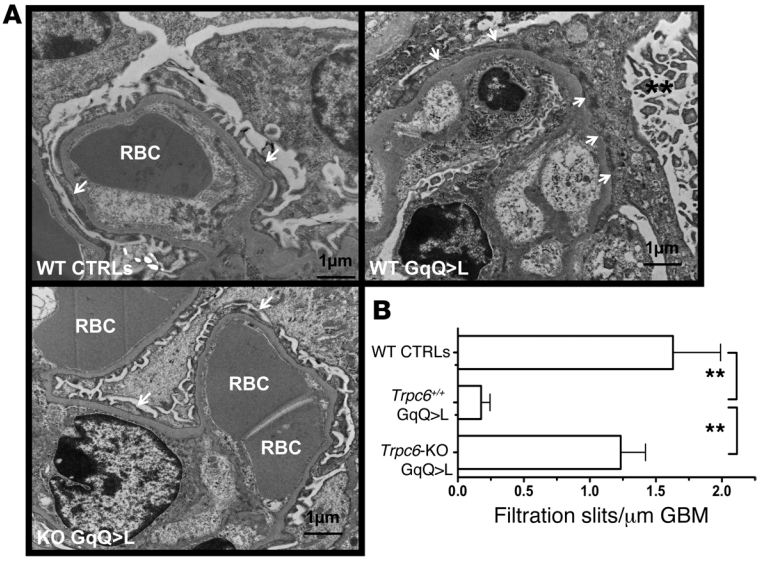


**Figure 5. Effect of *Trpc6* KO on glomerular ultrastructure.** (**A**) FP effacement was observed in all groups of PAN-treated mice (arrows), but was qualitatively more severe in *Trpc6*$^{+/+}$ GqQ>L mice treated with PAN. Microvillous changes were observed in a few *Trpc6*$^{+/+}$ GqQ>L mice (asterisks). Scale bars: 1 μm. (**B**) The number of filtration slits was significantly reduced in *Trpc6*$^{+/+}$ GqQ>L mice compared with that in either WT controls or *Trpc6*-KO GqQ>L mice. Red blood cells (RBC) are labeled in the capillary loops. For the experiments, 2–3 mice were studied in each group. $^{**}P < 0.05$ versus the indicated groups using ANOVA, followed by Bonferroni's post-hoc analysis.

rectly contributes to RTC injury by causing protein overload and apoptosis of RTCs. In this scenario, CN inhibition might attenuate tubular damage by both reducing proteinuria and inhibiting podocyte apoptosis in proteinuric renal diseases.

While off-target actions may have limited the beneficial effects of CN inhibition in the current study, KO of *Trpc6* attenuated both glomerular and tubular damage, suggesting that TRPC6 might be an important therapeutic target for the treatment of glomerular diseases. These beneficial effects were associated with a reduction in expression of the CN gene target *Cox2*, consistent with the idea that some of the beneficial effects may have been mediated by reducing CN activity. In support of targeting TRPC6 for therapeutic benefit, AII-induced albuminuria is reduced in *Trpc6*-KO mice (37). Moreover, overexpression of TRPC6 in podocytes promotes proteinuria and glomerulosclerosis in mice (71). In contrast, TRPC6 protected podocytes from complement-mediated glomerular disease (72). Thus, the effects of TRPC6 in glomerular disease processes are context dependent, which has important implications if TRPC6 inhibitors are developed for the treatment of glomerular diseases.

To determine whether the adverse effects of podocyte Gq activation were generalizable to other glomerular disease processes, we investigated the effect of GqQ>L induction on diabetic kidney disease in Akita mice. The rationale for studying Gq activation in this model is based on the observations that: (a) the renin-angiotensin system is a disease accelerant in rodent models of diabetic kidney disease (39, 40); and (b) the beneficial actions of AT1 receptor blockers in diabetic nephropathy are mediated by blocking the Gq-coupled AT1 receptor (8, 9). In this scenario, signaling cascades activated by Gq may provide the second hit that augments kidney damage in diabetic kidney disease. In support of this hypothesis, induction of GqQ>L promoted albuminuria, enhanced mesangial expansion, and increased GBM width in Gq Akita mice compared with WT Akita animals. In WT Akita mice, the diabetic milieu was also associated with a significant increase in expression of mRNA for the CN-responsive genes *Trpc6* ($P < 0.05$) and *Rcan1* ($P < 0.01$), consistent with published studies suggesting that renal CN activity is enhanced in rodent models of diabetes (23, 73). Surprisingly, induction of GqQ>L was not associated with a significant increase in mRNA for either *Trpc6* or *Rcan1*. We speculate that these observations are the result of compensatory mechanisms that limit the duration of Gq activation, including enhanced expression of the negative regulator of Gq signaling RGS2 (regulation of G protein signaling 2) (74) and modulation of IP3 receptor expression and activity (75, 76). In support of this hypothesis, IP3 receptor expression tended to be decreased in both groups of Akita mice compared with that in controls, and RGS2 levels tended to be higher in Gq Akita mice compared with those in WT Akita mice (Supplemental Figure 10). Regulation of Gq-dependent calcium signaling is, however, complex and includes not only modulation of mRNA and protein levels of the downstream signaling molecules, but also posttranslational modifications, accessory proteins, and proteasomal degradation (74–77). These regulatory mechanisms are an ongoing and evolving area of investigation, as they are incompletely understood. Further study will be required to better understand these counterregulatory pathways.

In the present study, systemic BP was similar in *Trpc6*$^{+/+}$ GqQ>L and *Trpc6*-KO GqQ>L mice. This finding contrasts with the higher systemic BP reported by Dietrich et al. (78) in the initial description of *Trpc6*-KO mice. While we can only speculate on the reason for this difference, genetic background may play a role. In the study by Dietrich et al. (78), the mice were on a mixed 129Sv/C56BL/6J background; in the present study, the mice were on an inbred FVB/NJ background. Consistent with an effect of genetic background on the BP phenotype, Eckel et al. (37) reported no differences in systemic BP by either tail-cuff manometry or radiotelemetry in mice on an inbred 129SvEv background. Moreover, a significant increase in systemic BP would likely have minimized the beneficial effects of *Trpc6*-KO in the PAN nephrosis model, given the adverse effect of increased BP on the progression of kidney disease

Finally, glomerular disease in mice is generally less severe compared with glomerular disease processes in other rodent models (45). Thus, the lack of a phenotype in GqQ>L mice might not be generalizable to other species. In addition, the adverse effects of Gq activation in the present study are likely cell-type specific. With regard to the latter, P2Y2 purinergic receptors are potent activators of TRPC6 in podocytes (46, 79), but whole-body KO of the gene encoding the P2Y2 receptor was found to aggravate kidney injury following subtotal nephrectomy (80). In that study, the authors attributed the adverse effects of P2Y2 KO to higher systemic BP and ineffective compensatory hypertrophy (80). Indeed, the P2Y2 receptor has complex effects on salt and water metabolism (81)

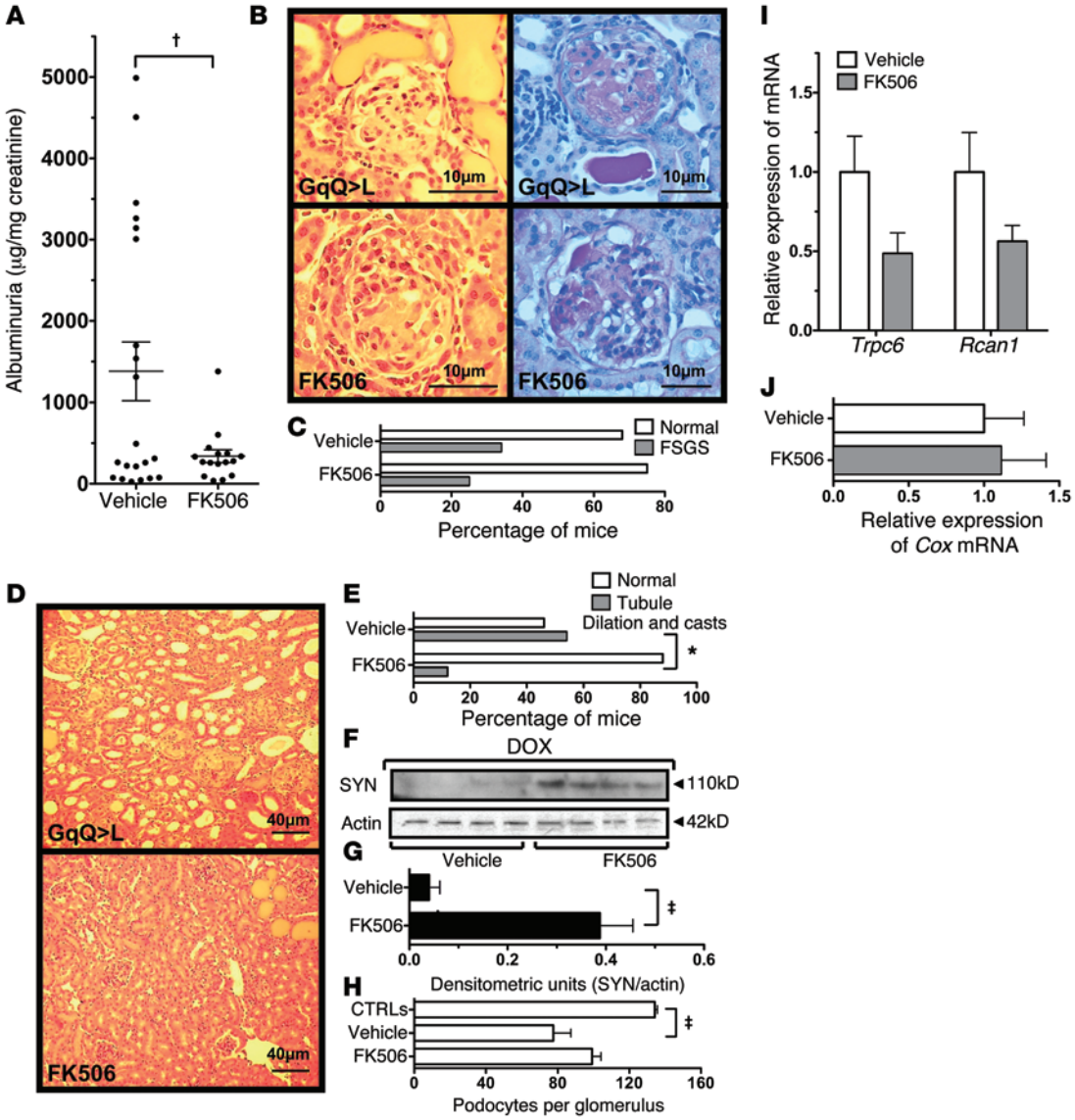


**Figure 6. Effect of CN inhibition on PAN nephrosis in GqQ>L mice.** (**A**) FK506 inhibited albuminuria induced by PAN in GqQ>L mice. (**B** and **C**) The development of FSGS was similar in GqQ>L mice treated with either vehicle or FK506. Scale bars: 10 μm. (**D** and **E**) FK506 significantly inhibited tubule dilation and casts. Scale bars: 40 μm. (**F** and **G**) FK506 significantly preserved SYN expression. (**H**) PAN nephrosis significantly reduced podocyte numbers in GqQ>L mice treated with vehicle compared with those in an untreated non-Tg control group. FK506 caused a modest and nonsignificant increase in podocyte numbers. (**I**) FK506 tended to reduce expression of the CN-responsive genes *Trpc6* and *Rcan1*. (**J**) The increase in *Cox2* mRNA caused by induction of GqQ>L (Figure 4I) was not affected by FK506. For the albuminuria studies, 16 vehicle-treated mice and 21 mice treated with FK506 were used. Sixteen vehicle-treated mice and 8 mice treated with FK506 were used for the histologic studies. For the immunoblot studies, 4 vehicle-treated mice and 4 mice treated with FK506 were used. To assess podocyte numbers, 11 untreated controls, 13 GqQ>L mice treated with vehicle, and 8 GqQ>L mice treated with FK506 were used. For qRT-PCR, mRNA samples from 14 vehicle-treated mice and 7 mice treated with FK506 were used. $^{*}P < 0.05$, $^{\dagger}P < 0.025$, or $^{\ddagger}P < 0.01$ versus the indicated groups using Fisher's exact test for histologic data, a 2-tailed *t* test for albuminuria and immunoblotting data, and ANOVA, followed by Bonferroni's post-hoc analysis, for the other studies.

that caused a significant increase in systolic BP following subtotal nephrectomy compared with that in WT animals (80). Additional studies will therefore be required to determine whether targeting Gq signaling using pharmacologic agents is a potentially beneficial strategy for treating glomerular disease processes.

In summary, we found that induction of GqQ>L specifically in podocytes caused robust albuminuria, FP effacement, decreased numbers of glomerular podocytes, and light microscopic features of FSGS. Moreover, Gq activation stimulated CN activity and upregulated TRPC6 expression in a CN-dependent fashion. KO of *Trpc6* ameliorated albuminuria, FP effacement, and the decrease in glomerular podocyte numbers as well as prevented the development of FSGS and inhibited tubular injury. CN inhibition had similar beneficial effects on albuminuria, but was less effective in reducing renal histologic damage. Taken together, these data suggest that components of the Gq/CN/TRPC6 signaling cascade are important therapeutic targets for the treatment of FSGS and likely other glomerular disease processes. In support of the latter,

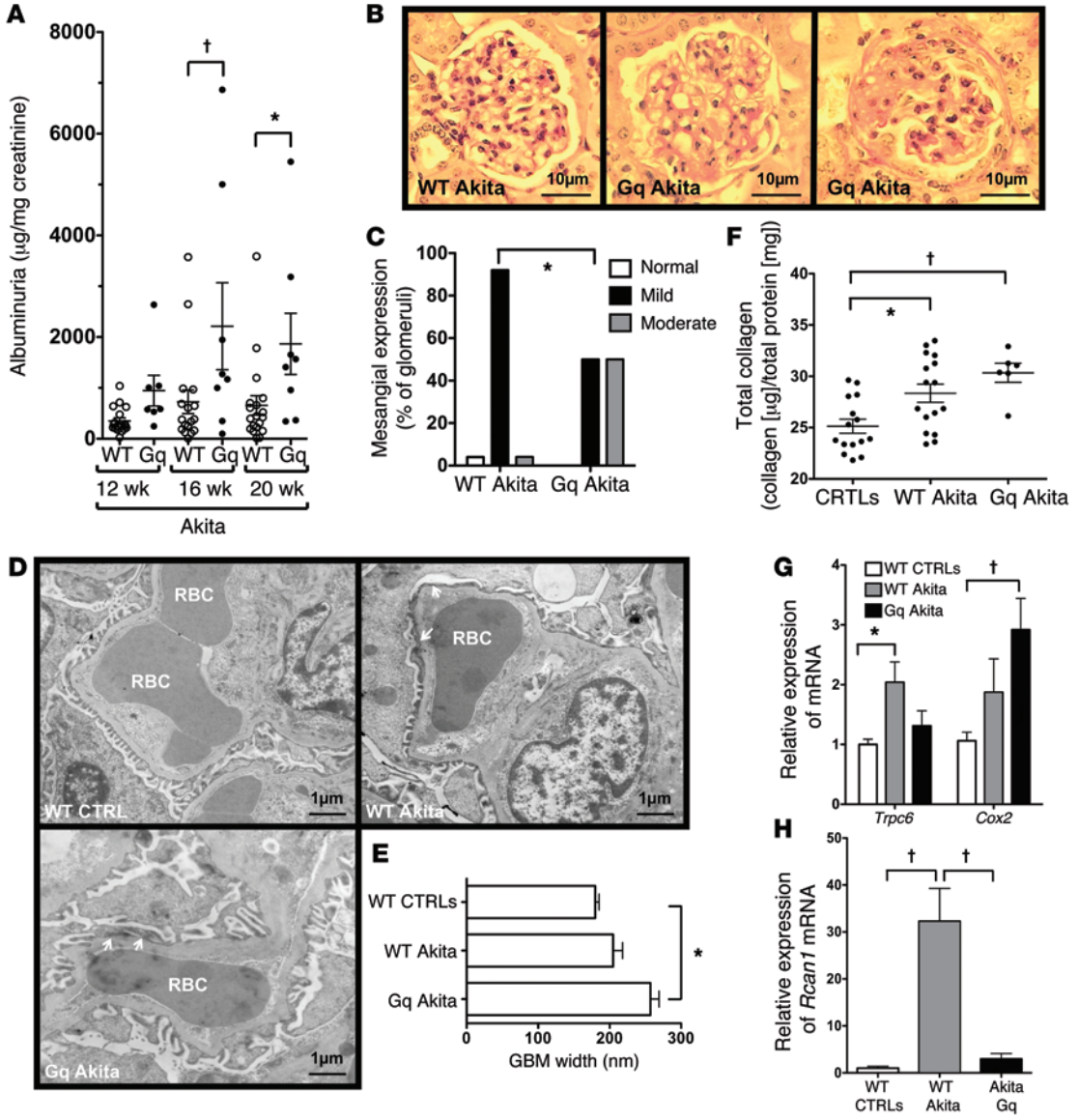


**Figure 7. Effect of GqQ>L on diabetic kidney disease.** (**A**) Albuminuria was enhanced at 16 and 20 weeks of age in Akita mice expressing GqQ>L (Gq Akita mice). (**B** and **C**) Mesangial expansion was increased in Gq Akita mice. Scale bars: 10 μm. (**D** and **E**) Nodular, subepithelial thickening of the GBM was seen in Gq Akita mice, which was associated with an increase in average GBM width. Focal areas of FP flattening were also observed (arrows). (**F**) Total collagen content was increased in both groups of Akita mice. (**G** and **H**) *Trpc6* and *Rcan1* mRNA levels were increased in glomerular preparations from WT Akita mice. *Cox2* mRNA was increased in Gq Akita mice. In contrast, mRNA levels for *Trpc6* and *Rcan1* were decreased in Gq Akita mice compared with levels in WT Akita mice. For the albuminuria and histologic studies, 18 WT Akita mice and 8 Gq Akita mice were used. For the collagen studies, 16 WT Akita mice, 7 Gq Akita mice, and 15 nondiabetic age- and sex-matched controls were used. Three WT Akita mice, 2 Gq Akita mice, and 3 WT controls were used for the TEM studies. For qRT-PCR, samples from 13 WT controls, 16 WT Akita mice, and 7 Gq Akita mice were used. Red blood cells are labeled in the capillary loops. $^{*}P < 0.05$ or $^{\dagger}P < 0.01$ versus the indicated groups using Fisher's exact test for mesangial expansion data and ANOVA, followed by Bonferroni's post-hoc analysis, for the other studies.

the adverse effects of podocyte Gq activation were generalizable to diabetic kidney disease in a mouse model of type 1 diabetes. Moreover, the data support the concept that a second hit may be required for the development of some familial forms of FSGS such as gain-of-function mutations in *TRPC6*.

## Methods

*Materials*. PAN was obtained from Sigma-Aldrich. Injectable FK506 (Astellas Pharma) was obtained from the Duke University Medical Center Pharmacy. The *tetO*-GqQ>L Tg mice were created as previously described (28). Podocin promoter *rtTA* Tg mice were originally obtained from Jeffery Kopp (33) at the NIH and are now available through The Jackson Laboratory. *Trpc6*-KO mice were obtained from Lutz Birnbaumer (78) through a collaboration with Michelle Winn.

*Experimental protocol*. All experiments were performed using mice backcrossed onto an FVB/NJ background for more than 10 generations. In pilot studies, age- and sex-matched 3- to 4-month-old littermates received DOX in their drinking water (with 2% sucrose to enhance palatability) for 1 week, and then nephrosis was induced by a single i.p. injection of PAN (500 mg/kg) as previously described (34). DOX was continued for the next 2 weeks, and urine was collected on the day prior to the PAN injection (day 0) and on days 7, 10, 14, and 28

after injection. As shown in Supplemental Figure 11, these pilot studies suggested that the most robust albuminuria occurred 10 days after PAN injection in GqQ>L mice. For the FSGS studies, we therefore collected urine on days 0 and 10. Mice were sacrificed and their kidneys harvested for examination by light microscopy, transmission electron microscopy (TEM), and fluorescence microscopy and for preparation of enriched glomerular preparations as previously described (28).

To determine the role of TRPC6 in PAN nephrosis, *Trpc6*-KO mice (*Trpc6*$^{-/-}$ mice) were bred onto an FVB background for more than 10 generations and then crossed with *tetO-rtTA* and *NPHS2* GqQ>L mice. Heterozygous offspring were then bred to create both double-Tg mice lacking *Trpc6* as well as controls (single-Tg and non-Tg *Trpc6*$^{-/-}$ mice). Mice were then studied using the PAN protocol described above.

To determine the role of CN in PAN nephrosis, GqQ>L mice were treated with an injectable form of FK506 by diluting the drug in saline (0.9% sodium chloride) and then administering twice-daily s.c. injections of either saline vehicle or 10 mg/kg/day FK506 beginning the day of PAN treatment and continuing until harvest. Mice were then studied using the PAN protocol described above.

For the NFAT reporter studies, *NPHS2-rtTA* mice and *tetO*-GqQ>L mice were bred with mice expressing an NFAT-responsive promoter driving expression of β-gal (36) to create mice with 2 different transgenes. Double-Tg offspring were then bred to create mice that expressed all 3 transgenes. In these triple-Tg mice, treatment with DOX induced GqQ>L and activated CN, which promoted expression of β-gal. Controls included double- and single-Tg mice (labeled "other Tg" mice) as well as non-Tg animals. To measure NFAT promoter activity, cortical and glomerular homogenates were prepared, and β-gal activity was measured using the Galacto-Star Chemiluminescent Reporter Gene Assay (Applied Biosystems). Data are expressed as β-gal activity per milligram protein.

To determine the effect of GqQ>L induction on TRPC6 expression in vivo, mice expressing GqQ>L and control mice were treated for 1 week with DOX in the drinking water, and then enriched glomerular preparations were prepared as previously described (28). The glomerular preparations were then either: (a) snap-frozen in liquid nitrogen and saved at –70°C for preparation of total cellular RNA; or (b) solubilized in NP-40 lysis buffer (50 mM Tris-HCl, 150 mM sodium chloride, 2 mM EDTA, 1% IGEPAL CA-630 [NP-40]) with protease inhibitors (Sigma-Aldrich) by sonication and frozen at –70°C for immunoblot analysis. In some studies, mice received 10 mg/kg/day FK506 or vehicle, as described above, during the DOX administration.

For the Akita studies, FVB/NJ Akita mice (41) were bred with both FVB/NJ *tetO*-GqQ>L mice and *NPHS2-rtTA* mice to create double-Tg FVB/NJ Akita animals using male Akita mice and nondiabetic female mice, because fertility is reduced in diabetic mothers (9.4 ± 2.4 [nondiabetic] vs. 5.8 ± 2.8 [diabetic] pups/litter; $P < 0.001$). For the studies, only male mice were examined, because kidney disease is mild in diabetic female animals (41). Age- and sex-matched single-Tg Akita and non-TG Akita mice were used as controls. For these studies, the transgene was induced by daily s.c. injections of the DOX analog anhydrotetracycline (10 mg/kg; Cayman Chemical) to avoid potential problems of giving DOX in sucrose water to diabetic mice and to standardize the drug dosage. Moreover, DOX may have beneficial effects in diabetes (82), perhaps by inhibiting MMP activity (82). In contrast, anhydrotetracycline has minimal MMP inhibitory effects (82). Treatment with anhydrotetracycline was initiated in mice at 4 weeks of age, and urine was collected at 12, 16, and 20 weeks of age. Mice were then sacrificed and kidneys harvested for examination by light microscopy, TEM, and fluorescence microscopy and for preparation of enriched glomerular preparations.

*Isolation of mouse glomeruli*. Enriched glomerular preparations were prepared using previously described methods (28). Portions of the glomerular pellet were then used to either: (a) prepare total cellular RNA using the TRIzol reagent according to the the manufacturer's directions (Life Technologies); or (b) solubilize in NP-40 lysis buffer (50 mM Tris-HCl, 150 mM NaCl, 2 mM EDTA, 1% IGEPAL CA-630 [NP-40]) with protease inhibitors (Sigma-Aldrich) by sonication. RNA and protein samples were then frozen at –70°C. By light microscopy, the purity of the glomerular preparations ranged from 60% to 70%.

*Reverse transcription followed by qPCR*. Total cellular RNA was prepared using glomerular preparations and TRIzol reagent (Life Technologies) according to the manufacturer's directions . RNA was treated with RNAase-free DNAase (QIAGEN) and then reverse transcribed with SuperScript Reverse Transcriptase (Invitrogen) and oligo (dT) primers. Real-time quantitative PCR was performed using an iCycler (Bio-Rad) and the universal SYBR Green PCR Master Mix Kit (Applied Biosystems, Life Technologies). The amplification signals were normalized to endogenous cyclophilin mRNA levels. The primer sequences used for qRT-PCR can be found in the Supplemental Methods.

*Immunoblot analysis*. Immunoblotting was performed as previously described (28) using the Invitrogen Bis-Tris mini-gel system and the following Abs: (a) a mouse mAb against SYN (catalog 65194; Progen Biotechnik); (b) a mouse mAb against WT1 (immunoblotting) (catalog sc-7385; Santa Cruz Biotechnology Inc.); and (c) a rabbit polyclonal Ab against TRPC6 (catalog ACC-017; Alomone Labs). As a positive control for the TRPC6 immunoblotting experiments, human embryonic kidney cells (HEK293 cells) were obtained from the Duke Cell Culture Facility and were transfected with a *TRPC6* cDNA (83). HEK293 cell lysates were then prepared using NP-40 lysis buffer. To assess protein loading, the immunoblots were stripped according to the manufacturer's instructions, and immunoblotting was performed using a mouse mAb against β-actin (catalog MAB1501R; Chemicon International). For densitometry, the immunoblots were converted into a digital format using an Epson Perfection 1670 Scanner (Seiko Epson) and then analyzed using ScanAnalysis 2.5 software (Biosoft). Densitometric data were normalized by dividing the protein signals for TRPC6, SYN, or WT1 by the matched signal for β-actin. When multiple blots were required to analyze a large number of samples, all gels were run and transferred simultaneously to PVDF membranes. The proteins were then detected by immunoblotting using the Abs described above. For these studies, ECL (Thermo Scientific) was performed by placing all PDVF membranes into a film cassette and exposing the x-ray film to all immunoblots for the same duration. The full, uncut gels are shown in the supplemental material.

*IHC*. Mouse kidney cortex was embedded in OCT compound, snap-frozen in liquid nitrogen, and stored at –70°C until sectioning. Expression of SYN and WT1 was identified by indirect immunofluorescence using a mouse mAb against SYN (catalog 65194; Progen Biotechnik), a rabbit polyclonal Ab against WT1 (catalog sc-192; Santa Cruz Biotechnology Inc.), or a rat mAb (clone 3F10) against the HA tag in the GqQ>L construct (catalog 11-867-423-001; F. Hoffmann-La Roche). Briefly, frozen sections were fixed in 2% paraformaldehyde for 10 minutes, air dried, treated for 10 minutes with 1% Triton-X in Dulbecco's

PBS (D-PBS), and then blocked for 1 hour in 20 mM Tris-HCl, 137 mM NaCl, pH 7.6 (TBS), with 0.2% Tween-20 (T-TBS) and 5% nonfat dry milk. The SYN, WT1, and HA Abs were added at a dilution of 1:200 in T-TBS with 5% nonfat dry milk. After incubating overnight, slides were washed 3 times in D-PBS and then incubated for 1 hour with either an Alexa Fluor 488 donkey anti-rabbit Ab (catalog A21206; Life Technologies), a goat CY3 anti-rat Ab (catalog A10522; Life Technologies), a rhodamine-labeled goat anti-mouse Ab (catalog R6393; Life Technologies), or a fluoresceinated donkey anti-mouse Ab (catalog ab98554; Abcam), all at a dilution of 1:1,000 in T-TBS with 5% nonfat dry milk. Slides were then washed 3 times in D-PBS, coverslips were applied using adhesive containing DAPI, and slides were examined using a Nikon Eclipse TE2000-S fluorescence microscope.

*BP measurements*. Systolic BP was measured using a computerized tail-cuff system (Hatteras Instruments) in conscious mice as previously described (34). This technique has previously been shown to correlate closely with intra-arterial measurements (84).

*Histopathology*. Light microscopic sections were stained with H&E and periodic acid Schiff (PAS) and then evaluated by a pathologist (A.F. Buckley) blinded to the genotype. FSGS, tubule dilation and casts, and TI inflammation and fibrosis were graded using a semiquantitative scale of 0 to 3 (0 = normal, 1 = mild, 2 = moderate, 3 = severe). For the Akita studies, mesangial expansion was assessed using the same grading scale as that described previously (41).

*Albuminuria*. Urine was collected for 24 hours in metabolic cages specifically designed for collection of urine in mice (Hatteras Instruments). Urinary albumin concentrations were measured using a kit from AssayPro, and urine creatinine levels were measure using a kit from Exocell. Urinary albumin excretion was expressed as both the albumin excretion rate per 24 hours and the albumin/creatinine ratio.

*TEM and GBM width analyses*. TEM was performed as previously described (55) at the Duke Electron Microscopy Core Facility. Analysis at the ultrastructural level was performed in a qualitative fashion, and areas of interest were selected in semithin sections for preparation of ultrathin sections to be examined by a pathologist (A.F. Buckley) blinded to the genotype. Digital images (3 animals from each group) were analyzed for density of patent slit diaphragms using Adobe Photoshop CS6 Extended Software (Adobe Systems) as previously described (34). Data were expressed as the number of patent slit diaphragms per micrometer of GBM length.

*Quantitation of GBM width, podocyte numbers, podocyte density, and glomerular volume*. See the Supplemental Methods.

*Statistics*. Data are presented as the mean ± SEM, and statistical analyses were performed using Prism software, version 5.0 (GraphPad Software). For comparison of continuous variables, a Kolmogorov-Smirnov test of normality was performed prior to assessing statistical significance using the following statistical methods: (a) a 2-tailed *t* test for variables passing the normality test; or (b) a Mann-Whitney *U* test for variables that were not normally distributed. For comparisons between more than 2 groups, statistical analysis included either: (a) a 1-way ANOVA, followed by a Bonferroni's multiple comparisons post test for normally distributed variables; or (b) a Kruskal-Wallis test, followed by a Dunn's multiple comparisons post test for variables that were not normally distributed. For noncontinuous variables, data were calculated using either Fisher's exact test or $\chi^2$ analysis. Histologic data were analyzed as a noncontinuous variable using the number of mice with the specified histologic abnormality. *P* values of less than 0.05 were considered significant. Graphs of the histologic findings are presented as the percentage of mice with the specified abnormality to permit a more effective comparison of the differences between the experimental manipulations in studies with an imbalance in the number of mice in each group.

*Study approval*. All animal care and experiments conformed to NIH guidelines (*Guide for the Care and Use of Laboratory Animals*. 8th ed. The National Academies Press. 2011.) and were approved by the IACUC of the Duke University Medical Center.

## Acknowledgments

These studies were supported by grants from the NIH (R01-DK075688 and R01-DK087707, to R.F. Spurney); the Veterans Administration Merit Review Program (BX000791, to R.F. Spurney); and by a Department of Medicine Integrated Research Award through an internal grant program at Duke University Medical Center (to P.B. Rosenberg and R.F. Spurney). We thank Natalie Mattocks and William Eisner for their technical assistance with the studies.

Address correspondence to: Robert F. Spurney, MSRB II, Room 2013, 106 Research Drive, Durham, North Carolina 27710, USA. Phone: 919.684.9729; E-mail: robert.spurney@dm.duke.edu.

1. Winn MP, Daskalakis N, Spurney RF, Middleton JP. Unexpected role of TRPC6 channel in familial nephrotic syndrome: does it have clinical implications? *J Am Soc Nephrol*. 2006;17(2):378–387.
2. Pavenstädt H. Roles of the podocyte in glomerular function. *Am J Physiol Renal Physiol*. 2000;278(2):F173–F179.
3. Tian D, et al. Antagonistic regulation of actin dynamics and cell motility by TRPC5 and TRPC6 channels. *Sci Signal*. 2010;3(145):ra77.
4. Greka A, Mundel P. Balancing calcium signals through TRPC5 and TRPC6 in podocytes. *J Am Soc Nephrol*. 2011;22(11):1969–1980.
5. Pavenstadt H, Kriz W, Kretzler M. Cell biology of the glomerular podocyte. *Physiol Rev*. 2003;83(1):253–307.
6. Mitra SK, Hanson DA, Schlaepfer DD. Focal adhesion kinase: in command and control of cell motility. *Nat Rev Mol Cell Biol*. 2005;6(1):56–68.
7. Lewis EJ, Hunsicker LG, Bain RP, Rohde RD. The effect of angiotensin-converting-enzyme inhibition on diabetic nephropathy. The Collaborative Study Group. *N Engl J Med*. 1993;329(20):1456–1462.
8. Brenner BM, et al. Effects of losartan on renal and cardiovascular outcomes in patients with type 2 diabetes and nephropathy. *N Engl J Med*. 2001;345(12):861–869.
9. Lewis EJ, et al. Renoprotective effect of the angiotensin-receptor antagonist irbesartan in patients with nephropathy due to type 2 diabetes. *N Engl J Med*. 2001;345(12):851–860.
10. Kohan DE, et al. Addition of atrasentan to renin-angiotensin system blockade reduces albuminuria in diabetic nephropathy. *J Am Soc Nephrol*. 2011;22(4):763–772.
11. Mann JF, et al. Avosentan for overt diabetic nephropathy. *J Am Soc Nephrol*. 2010;21(3):527–535.
12. Wenzel RR, et al. Avosentan reduces albumin excretion in diabetics with macroalbuminuria. *J Am Soc Nephrol*. 2009;20(3):655–664.
13. Nishizuka Y. Intracellular signaling by hydrolysis of phospholipids and activation of protein kinase C. *Science*. 1992;258(5082):607–614.
14. Menne J, Meier M, Park JK, Haller H. Inhibition of protein kinase C in diabetic nephropathy — where do we stand? *Nephrol Dial Transplant*. 2009;24(7):2021–2023.
15. Winn MP, et al. A mutation in the TRPC6 cation channel causes familial focal segmental glomerulosclerosis. *Science*. 2005;308(5729):1801–1804.
16. Reiser J, et al. TRPC6 is a glomerular slit diaphragm-associated channel required for normal renal function. *Nat Genet*. 2005;37(7):739–744.

17. Möller CC, et al. Induction of TRPC6 channel in acquired forms of proteinuric kidney disease. *J Am Soc Nephrol*. 2007;18(1):29–36.
18. Rao A, Luo C, Hogan PG. Transcription factors of the NFAT family: regulation and function. *Annu Rev Immunol*. 1997;15:707–747.
19. Molkentin JD, et al. A calcineurin-dependent transcriptional pathway for cardiac hypertrophy. *Cell*. 1998;93(2):215–228.
20. Sussman MA, et al. Prevention of cardiac hypertrophy in mice by calcineurin inhibition. *Science*. 1998;281(5383):1690–1693.
21. Kuwahara K, et al. TRPC6 fulfills a calcineurin signaling circuit during pathologic cardiac remodeling. *J Clin Invest*. 2006; 116(12):3114–3126.
22. Faul C, et al. The actin cytoskeleton of kidney podocytes is a direct target of the antiproteinuric effect of cyclosporine A. *Nat Med*. 2008;14(9):931–938.
23. Wang L, Chang JH, Paik SY, Tang Y, Eisner W, Spurney RF. Calcineurin (CN) activation promotes apoptosis of glomerular podocytes both in vitro and in vivo. *Mol Endocrinol*. 2011;25(8):1376–1386.
24. Wang Y, et al. Activation of NFAT signaling in podocytes causes glomerulosclerosis. *J Am Soc Nephrol*. 2010;21(10):1657–1666.
25. Cayouette S, Lussier MP, Mathieu EL, Bousquet SM, Boulay G. Exocytotic insertion of TRPC6 channel into the plasma membrane upon Gq protein-coupled receptor activation. *J Biol Chem*. 2004;279(8):7241–7246.
26. Nijenhuis T, et al. Angiotensin II contributes to podocyte injury by increasing TRPC6 expression via an NFAT-mediated positive feedback signaling pathway. *Am J Pathol*. 2011;179(4):1719–1732.
27. Zhang H, Ding J, Fan Q, Liu S. TRPC6 up-regulation in Ang II-induced podocyte apoptosis might result from ERK activation and NF-κB translocation. *Exp Biol Med (Maywood)*. 2009;234(9):1029–1036.
28. Wang L, Flannery PJ, Rosenberg PB, Fields TA, Spurney RF. Gq-dependent signaling upregulates COX2 in glomerular podocytes. *J Am Soc Nephrol*. 2008;19(11):2108–2118.
29. D'Agati VD, Kaskel FJ, Falk RJ. Focal segmental glomerulosclerosis. *N Engl J Med*. 2011;365(25):2398–2411.
30. El Hindi S, Reiser J. TRPC channel modulation in podocytes-inching toward novel treatments for glomerular disease. *Pediatr Nephrol*. 2011;26(7):1057–1064.
31. Fogo AB. Animal models of FSGS: lessons for pathogenesis and treatment. *Semin Nephrol*. 2003;23(2):161–171.
32. Gingrich JR, Roder J. Inducible gene expression in the nervous system of transgenic mice. *Annu Rev Neurosci*. 1998;21:377–405.
33. Shigehara T, et al. Inducible podocyte-specific gene expression in transgenic mice. *J Am Soc Nephrol*. 2003;14(8):1998–2003.
34. Wang L, Ellis MJ, Fields TA, Howell DN, Spurney RF. Beneficial effects of the Rho kinase inhibitor Y27632 in murine puromycin aminonucleoside nephrosis. *Kidney Blood Press Res*. 2008;31(2):111–121.
35. Vassiliadis J, Bracken C, Matthews D, O'Brien S, Schiavi S, Wawersik S. Calcium mediates glomerular filtration through calcineurin and mTORC2/Akt signaling. *J Am Soc Nephrol*. 2011;22(8):1453–1461.
36. Rosenberg P, et al. TRPC3 channels confer cellular memory of recent neuromuscular activity. *Proc Natl Acad Sci U S A*. 2004;101(25):9387–9392.
37. Eckel J, et al. TRPC6 enhances angiotensin II-induced albuminuria. *J Am Soc Nephrol*. 2011;22(3):526–535.
38. Shirakawa H, et al. Transient receptor potential canonical 3 (TRPC3) mediates thrombin-induced astrocyte activation and upregulates its own expression in cortical astrocytes. *J Neurosci*. 2010;30(39):13116–13129.
39. Kelly DJ, Wilkinson-Berka JL, Allen TJ, Cooper ME, Skinner SL. A new model of diabetic nephropathy with progressive renal impairment in the transgenic (mRen-2)27 rat (TGR). *Kidney Int*. 1998;54(2):343–352.
40. Conway BR, et al. Hyperglycemia and renin-dependent hypertension synergize to model diabetic nephropathy. *J Am Soc Nephrol*. 2012;23(3):405–411.
41. Chang JH, et al. Diabetic kidney disease in FVB/NJ Akita mice: temporal pattern of kidney injury and urinary nephrin excretion. *PLoS One*. 2012;7(4):e33942.
42. Heeringa SF, et al. A novel TRPC6 mutation that causes childhood FSGS. *PLoS One*. 2009;4(11):e7771.
43. Gigante M, et al. TRPC6 mutations in children with steroid-resistant nephrotic syndrome and atypical phenotype. *Clin J Am Soc Nephrol*. 2011;6(7):1626–1634.
44. Tory K, et al. Mutation-dependent recessive inheritance of NPHS2-associated steroid-resistant nephrotic syndrome. *Nat Genet*. 2014;46(3):299–304.
45. Pippin JW, et al. Inducible rodent models of acquired podocyte diseases. *Am J Physiol Renal Physiol*. 2009;296(2):F213–F229.
46. Roshanravan H, Dryer SE. ATP acting through P2Y receptors causes activation of podocyte TRPC6 channels: role of podocin and reactive oxygen species. *Am J Physiol Renal Physiol*. 2014;306(9):F1088–F1097.
47. Anderson M, Roshanravan H, Khine J, Dryer SE. Angiotensin II activation of TRPC6 channels in rat podocytes requires generation of reactive oxygen species. *J Cell Physiol*. 2014;229(4):434–442.
48. Brandes RP, Weissmann N, Schroder K. Nox family NADPH oxidases: Molecular mechanisms of activation. *Free Radic Biol Med*. 2014;76:208–226.
49. Takasaki J, et al. A novel Gαq/11-selective inhibitor. *J Biol Chem*. 2004;279(46):47438–47445.
50. Uemura T, et al. Biological properties of a specific Gαq/11 inhibitor, YM-254890, on platelet functions and thrombus formation under high-shear stress. *Br J Pharmacol*. 2006;148(1):61–69.
51. Kawasaki T, et al. Pharmacological properties of YM-254890, a specific G(alpha)q/11 inhibitor, on thrombosis and neointima formation in mice. *Thromb Haemost*. 2005;94(1):184–192.
52. Berridge MJ, Lipp P, Bootman MD. The versatility and universality of calcium signalling. *Nat Rev Mol Cell Biol*. 2000;1(1):11–21.
53. Bollée G, et al. Epidermal growth factor receptor promotes glomerular injury and renal failure in rapidly progressive crescentic glomerulonephritis. *Nat Med*. 2011;17(10):1242–1250.
54. Plant TD, Schaefer M. TRPC4 and TRPC5: receptor-operated $Ca^{2+}$-permeable nonselective cation channels. *Cell Calcium*. 2003;33(5):441–450.
55. Wang L, et al. Mechanisms of the proteinuria induced by Rho GTPases. *Kidney Int*. 2012;81(11):1075–1085.
56. Zhu L, Jiang R, Aoudjit L, Jones N, Takano T. Activation of RhoA in podocytes induces focal segmental glomerulosclerosis. *J Am Soc Nephrol*. 2011;22(9):1621–1630.
57. Scott RP, et al. Podocyte-specific loss of Cdc42 leads to congenital nephropathy. *J Am Soc Nephrol*. 2012;23(7):1149–1154.
58. Blattner SM, et al. Divergent functions of the Rho GTPases Rac1 and Cdc42 in podocyte injury. *Kidney Int*. 2013;84(5):920–930.
59. Schaldecker T, et al. Inhibition of the TRPC5 ion channel protects the kidney filter. *J Clin Invest*. 2013;123(12):5298–5309.
60. Schlöndorff J, Del Camino D, Carrasquillo R, Lacey V, Pollak MR. TRPC6 mutations associated with focal segmental glomerulosclerosis cause constitutive activation of NFAT-dependent transcription. *Am J Physiol Cell Physiol*. 2009;296(3):C558–C569.
61. Klein M, Radhakrishnan J, Appel G. Cyclosporine treatment of glomerular diseases. *Annu Rev Med*. 1999;50:1–15.
62. Mathieson PW. Proteinuria and immunity — an overstated relationship? *N Engl J Med*. 2008;359(23):2492–2494.
63. Parving HH, et al. Cardiorenal end points in a trial of aliskiren for type 2 diabetes. *N Engl J Med*. 2012;367(23):2204–2213.
64. Gaston RS. Chronic calcineurin inhibitor nephrotoxicity: reflections on an evolving paradigm. *Clin J Am Soc Nephrol*. 2009;4(12):2029–2034.
65. Naesens M, Kuypers DR, Sarwal M. Calcineurin inhibitor nephrotoxicity. *Clin J Am Soc Nephrol*. 2009;4(2):481–508.
66. Moran K, et al. Morphological changes and alterations in regional intrarenal blood flow induced by graded renal ischemia. *J Urol*. 1992;148(2):463–466.
67. Noguchi H, et al. A new cell-permeable peptide allows successful allogeneic islet transplantation in mice. *Nat Med*. 2004;10(3):305–309.
68. Aramburu J, Yaffe MB, López-Rodríguez C, Cantley LC, Hogan PG, Rao A. Affinity-driven peptide selection of an NFAT inhibitor more selective than cyclosporin A. *Science*. 1999;285(5436):2129–2133.
69. Cho SG, Du Q, Huang S, Dong Z. Drp1 dephosphorylation in ATP depletion-induced mitochondrial injury and tubular cell apoptosis. *Am J Physiol Renal Physiol*. 2010;299(1):F199–F206.
70. Li X, et al. PKC-Δ promotes renal tubular cell apoptosis associated with proteinuria. *J Am Soc Nephrol*. 2010;21(7):1115–1124.
71. Krall P, et al. Podocyte-specific overexpression of wild type or mutant trpc6 in mice is sufficient to cause glomerular disease. *PLoS One*. 2010;5(9):e12859.
72. Kistler AD, et al. Transient receptor potential channel 6 (TRPC6) protects podocytes during

complement-mediated glomerular disease. *J Biol Chem*. 2013;288(51):36598–36609.
73. Gooch JL, Barnes JL, Garcia S, Abboud HE. Calcineurin is activated in diabetes and is required for glomerular hypertrophy and ECM accumulation. *Am J Physiol Renal Physiol*. 2003;284(1):F144–F154.
74. Zhang P, Mende U. Functional role, mechanisms of regulation, and therapeutic potential of regulator of G protein signaling 2 in the heart. *Trends Cardiovasc Med*. 2014;24(2):85–93.
75. Mizuno K, Kurokawa K, Ohkuma S. Regulatory mechanisms and pathophysiological significance of IP3 receptors and ryanodine receptors in drug dependence. *J Pharmacol Sci*. 2013;123(4):306–311.
76. Foskett JK, White C, Cheung KH, Mak DO. Inositol trisphosphate receptor $Ca^{2+}$ release channels. *Physiol Rev*. 2007;87(2):593–658.
77. Umemori H, et al. Activation of the G protein Gq/11 through tyrosine phosphorylation of the α subunit. *Science*. 1997;276(5320):1878–1881.
78. Dietrich A, et al. Increased vascular smooth muscle contractility in $TRPC6^{-/-}$ mice. *Mol Cell Biol*. 2005;25(16):6980–6989.
79. Wilson C, Dryer SE. A mutation in TRPC6 channels abolishes their activation by hypoosmotic stretch but does not affect activation by diacylglycerol or G protein signaling cascades. *Am J Physiol Renal Physiol*. 2014;306(9):F1018–F1025.
80. Potthoff SA, et al. P2Y2 receptor deficiency aggravates chronic kidney disease progression. *Front Physiol*. 2013;4:234.
81. Vallon V, Rieg T. Regulation of renal NaCl and water transport by the ATP/UTP/P2Y2 receptor system. *Am J Physiol Renal Physiol*. 2011;301(3):F463–F475.
82. Ryan ME, Ramamurthy NS, Sorsa T, Golub LM. MMP-mediated events in diabetes. *Ann N Y Acad Sci*. 1999;878:311–334.
83. Hall G, et al. Phosphodiesterase 5 inhibition ameliorates angiontensin II-induced podocyte dysmotility via the protein kinase G-mediated downregulation of TRPC6 activity. *Am J Physiol Renal Physiol*. 2014;306(12):F1442–F1450.
84. Whitesall SE, Hoff JB, Vollmer AP, D'Alecy LG. Comparison of simultaneous measurement of mouse systolic arterial blood pressure by radiotelemetry and tail-cuff methods. *Am J Physiol Heart Circ Physiol*. 2004;286(6):H2408–H2415.